Article

Cross-Tier Interference Mitigation for RIS-Assisted Heterogeneous Networks

Abdel Nasser Soumana Hamadou[1]*, Ciira wa Maina[2], and Moussa Moindze Soidridine[3]

[1] Department of Electrical Engineering, PanAfrican University Institute for Basic Science, Technology, and Innovation (PAUSTI), Nairobi, Kenya.
[2]Centre for Data Science and Artificial Intelligence (DSAIL), Dedan Kimathi University of Technology, Nyeri, Kenya.
[3]Faculty of Science and Techniques, University of Comoros, Moroni, Comoros.
*Correspondence; nasser.abdel@students.jkuat.ac.ke

Abstract: New research issues have emerged with the development of the next generation of wireless networks, and new technologies have been proposed to address them. On the other hand, reconfigurable intelligent surface (RIS) technology is being looked into for controlling some aspects wireless channels. RIS is a promising technology for increasing signal quality by passively managing the dispersion of electromagnetic. Heterogeneous networks (HetNet) are a promising new technology created to satisfy the network's capacity needs. In the context of HetNet, RIS technology can be used to enhance system performance. This study investigates the applications of reconfigurable intelligent surfaces (RIS) in heterogeneous downlink networks (HetNet). Due to the network densification, the small cell base station (SBS) interferes with the macrocell users (MUE). In this paper, we utilize RIS to mitigate cross-tier interference in an HetNet via directional beamforming by adjusting the RIS's phase shift. We consider an RIS-assisted HetNet consisting of multiple SBS nodes and MUEs that utilize both direct paths and reflected paths. Therefore, the aim of this study is to maximize the sum rate of all MUEs by jointly optimizing the transmit beamforming of the macrocell base station (MBS) and the phase shift of the RIS. An efficient RIS reflecting coefficient-based optimization (RCO) is proposed based on a successive convex approximation approach. Simulation results are provided to show the effectiveness of the proposed scheme in terms of its sum rate in comparison with the scheme HetNet without RIS and the scheme HetNet with RIS but with random phase shifts.

Keywords: RIS; HetNet; Spectral Efficiency; Cross-tier Interference; Optimization; MIMO

1. Introduction

Future wireless communications will enable massive connectivity for mobile and fixed devices, which will require high demand for mobile data traffic on cellular networks in terms of data throughput and network capacity [1]. In order to respond to the requirements of high transmission rate and quality of services (QoS) for 5G systems, multitier networks improve the spectrum efficiency and capacity of the systems by adopting a heterogenous design with small cells and a macro cell tier [2]. High spectrum efficiency (SE) is necessary to enable smooth communication in heterogeneous network since the bandwidth resources become constrained as the number of cells grows [3]. Additionally, a multitier network with densely deployed cells experiences very high intercell interference as well as cross-tier interference, which may prevent the macrocell users (MUE) within the vicinity of the small base station (SBS) from having a good signal-to-interference-plus-noise ratio (SINR) as well as reduce the network's capacity overall [4]. Recently, business and academics have both shown a lot of interest in a developing hardware technology called reconfigurable intelligent surfaces (RISs), which aims to address the aforementioned challenge in heterogenous networks (HetNet) [5]– [11].

Specifically, RIS is a two-dimensional artificial surface made up of a variety of discrete parts that can be controlled individually or collectively [12]. It is a fresh approach to managing the wireless propagation medium, which was previously thought to be unmanageable.

Preprints (www.preprints.org) | NOT PEER-REVIEWED | Posted: 10 May 2023 doi:10.20944/preprints202305.0689.v1

RIS technologies are widely labelled in the literature under names like software-defined or hypersurfaces, intelligent walls, software-controlled metasurfaces, large intelligent surfaces or antennas, intelligent reflected surfaces (IRS), and reconfigurable intelligent surfaces. The implementation of an RIS-assisted system is identical to the use case for half-duplex relays with the important exception that RIS enables passive beamforming [13]. In this context, RIS-assisted communication can be used to improve the performance of traditional wireless communication systems by allowing more degrees of freedom via wireless channel control, resulting in a more relaxed set of constraints. Further, reconfigurable intelligent surfaces (RIS) can control the radio environment using low-noise amplification and do not require an analog, digital, or power amplifier [13]. An RIS can modify the phase shift, the amplitude, or even the polarization of the incident signal. Notably, the RIS technology is nearly passive in that it is entirely based on electromagnetic waves scattering and does require power amplifiers for signal transmission. Indeed, some energy is only required for the smart controller and for enabling the reconfigurability of the RIS. As a result, RIS can mitigate the interference or improve the signal quality at some specific and localized network locations. The RIS technology shows promising potential for applications in future networks, as it can partially control and shape the propagation channels as one desires. The deployment of RISs can be combined with existing technologies like multiple-input multiple-output (MIMO) systems, heterogeneous networks (HetNet) systems, millimetre-wave(mmWave) communications, terahertz (THz) communications, machine learning (ML), and artificial intelligence (AI) for enhancing the performance of existing and future wireless networks[12]–[14].

Furthermore, RIS technology can be applied in a heterogenous network to facilitate communications by creating additional propagation channel, improving the proprieties of the current paths, and reducing interference. Additionally, the components of a RIS are almost passive in that they passively filter incoming signals before passively reradiating them in the desired direction without the use of additional power. Additional characteristics of RISs include the following: RISs are passive system made primarily of low-cost materials. They can also be merely applied to factory ceilings, interior walls, and building facades because of how closely they resemble mirrors physically. The RIS has some of the most advantageous use cases for line-of-site (LOS) pathways or at the cell edge due to its capacity to rearrange signals [15], [16]. RIS does neither amplify or decode the incoming signal, unlike, conventional relaying methods like amplify-and-forward (AF) and decode-and forward (DF) relaying [15] and [17]. As a result, RIS contributes to the construction of a smart radio environment that may be adequately designed for inexpensive and energy-efficiency communication in HetNet by offering essential flexibility. However, in reality, adaptive phase shifting requires some active components.

2. Related works

The authors of [17] demonstrate that the RIS-aided transmission can outperform the DF relaying protocol in terms of EE for high-rate communications. However, the main advantage of RIS in HetNet is the algorithm structure for managing the phase changes of the passive elements.

By creating the phase shift controller utilizing alternating algorithm design, the authors of [18] examined a RIS-assisted cognitive radio (CR) communication strategy for optimizing the achievable secondary user (SU) rate of the system.

The authors of [6] designed a multi-eavesdropper multi-cast multiantenna optimization approach to analyse the RIS-assisted dual function radar communications (DFRC) scheme for maximizing the system's secrecy rate.

The performance of a single cell wireless system assisted by RIS with a multiantenna access point and multiple single antenna users was investigated by the authors in [10]. They focused on the asymptotic performance of RIS with an essentially unlimited of elements and contrasted it with a benchmark enormous multi-input multi-output (MIMO) system without RIS.

In [4], the authors developed an adaptative hybrid scheme technique that combined time domain technique using reduced power Almost Blank Subframe (ABS) and power control technique was then used to mitigate the cross-tier interference between the femto base station and the macrocell

 doi:10.20944/preprints202305.0689.v1

user near the femtocell. Results obtained from the simulation demonstrated that the proposed technique could increase the spectral efficiency of femtocells. The technique proposed in this study only considers cross-tier interference between the femto base station and macrocell users. Moreover, the energy efficiency of this technique was not considered as well.

In [19], the authors formulated a heuristic scheme called the Quality Efficient Femtocell Offloading Scheme (QEFOS), which classifies the users in three categories, namely, macrocell users which experience low cross-tier interference, macrocell users which experience high cross-tier interference, and femtocell users.

In [20], the authors proposed a method to mitigate downlink cross-tier interference between macro cell and small cells. The proposed method is based on an extended cross-tier interference mitigation scheme that coordinates not only cross-tier interference form macro cell to small cell users but also that from small cell to macro cell users, which consists to mitigate cross-tier interference from small cell to macro cell users without changing the pilot allocation.

In [21], the authors proposed a resource allocation scheme for RIS-assisted heterogeneous networks with non-orthogonal multiple access to improve spectrum efficiency and transmission rate. The proposed resource allocation scheme optimization is based on the alternating iteration approach and successive convex approximations. Nevertheless, this study did not consider the performance of the proposed method with respect to the user's location.

In [22], the authors investigated the performance of RIS-assisted wireless communication systems under co-channel interference in order to determine the closed-form expressions for the outage probability and channel capacity. However, this study did not actually take into consideration the RIS phase shift optimization as well as the trade-off between transmit power and co-channel interference.

In [23], the authors developed a novel scheme for efficient multiple access in RIS-aided multi-user multi-antenna systems. A comprehensive comparison of different schemes and configurations was presented in order to determine which scheme is better for the 6G paradigm. However, this study did not consider co-channel interference or the inter-user interference.

The study in [24] presented a survey of the design and applications of an RIS for beyond 5G wireless networks. A comprehensive, detailed survey of RIS technology limitations in current research and related research opportunities and possible solutions was presented.

In [25], the authors investigated the impact of the amplitude response on the capacity of a reconfigurable intelligent surface-enabled narrowband single-input single-output. Simulation results show a significant impact on the overall performance improvement of the system.

The study in [16] compared RIS-assisted system with the distributed antenna-aided system. However, the non-line-of-site link between the transmitter and receiver was no considered.

In [26], the authors investigate the intelligent reflecting surface (IRS) for sum-rate maximization in cognitive radio enabled wireless powered communications networks. They proposed an alternating (AO)-based solution with a successive convex approximation (SCA) technique to solve the unconvex optimization problem. Result conventional cognitive radio enabled wireless powered communications networks. Nevertheless, this study considers only cognitive radio enabled wireless powered communications networks.

Apart from cognitive radio (CR), MIMO, and DFRC communications, RIS have been used in D2D and IoT communication systems. For example, in [5], the authors analysed the performance of RIS-assisted IoT network using two resource allocation problems, namely, spectral efficiency and energy efficiency maximization. In [7], the authors investigated an RIS-based unmanned ariel vehicle (UAV) assisted non-orthogonal multiple access (NOMA) downlink scheme for maximizing the sum rate of the system by using a deep deterministic policy gradient (DDPG) algorithm.

However, except for the works in [19], [20] [21], and [22], where the authors proposed to mitigate cross-tier interference in HetNet without taking the impact of the users and RIS location in the network into consideration, because of this, a study of cross-tier interference mitigation in RIS-assisted HetNet is necessary, especially for maximising system sum rate and network performance with respect to user location and RIS location.

Preprints (www.preprints.org) | NOT PEER-REVIEWED | Posted: 10 May 2023 doi:10.20944/preprints202305.0689.v1

Therefore, in contrast to the aforementioned studies, in this work we examine a RIS-assisted HetNet where the reflected link from RIS to the macrocell users (MUE) as well as the reflected interference link form SBS-RIS-MUE are employed to mitigate interference from small cells (SBS). By optimizing the sum rate of the networks while keeping in mind the limitations of transmitting beamforming at the macrocell base station (MBS) and phase shift coefficients at the RIS, the main goal of this work is to develop an interference-aware heterogenous networks. The main contributions are outlined in the list below.

1. We investigate the maximization of spectrum efficiency in a RIS-assisted HetNet using a system model in which the macrocell base station (MBS) communicates with its users via a direct link and is reflected via RIS.
2. We investigate how RIS helps to resolve cross-tier interference issues in HetNet.
3. Because the formulated optimization problem is not convex, we resolve it by maximizing the sum rate of the combined desired channel by extending a semidefinite relaxation technique.
4. Finally, to confirm the viability of the suggested technique, numerical analysis is carried out through computer simulations under real-world channel conditions. To specifically measure and support the SE of the specified framework. The number of RIS elements, their location, and the number of SBS were all analyzed. Furthermore, we compare the proposed algorithm with HetNet without RIS and HetNet with RIS but with random phase shifts.

This paper is organized as follows: In section 2, we present some related works; next, in section 3, we describe the scheme model under study; then, in section 4, we formulate the problem and present the proposed optimisation method; and in section 5, the numerical and simulation results are presented, and finally, the paper concludes.

3. System Model

As shown in Fig. 1, we consider a RIS-assisted HetNet wireless network system that comprises K macro base station users (MUE) and M macro base station (MBS) antennas, where J SBS with S antennas are deployed under the overlaid MBS, and the MBS and users communicate via a RIS with N elements that reflects the incident signal into a direct channel and a reflected channel.

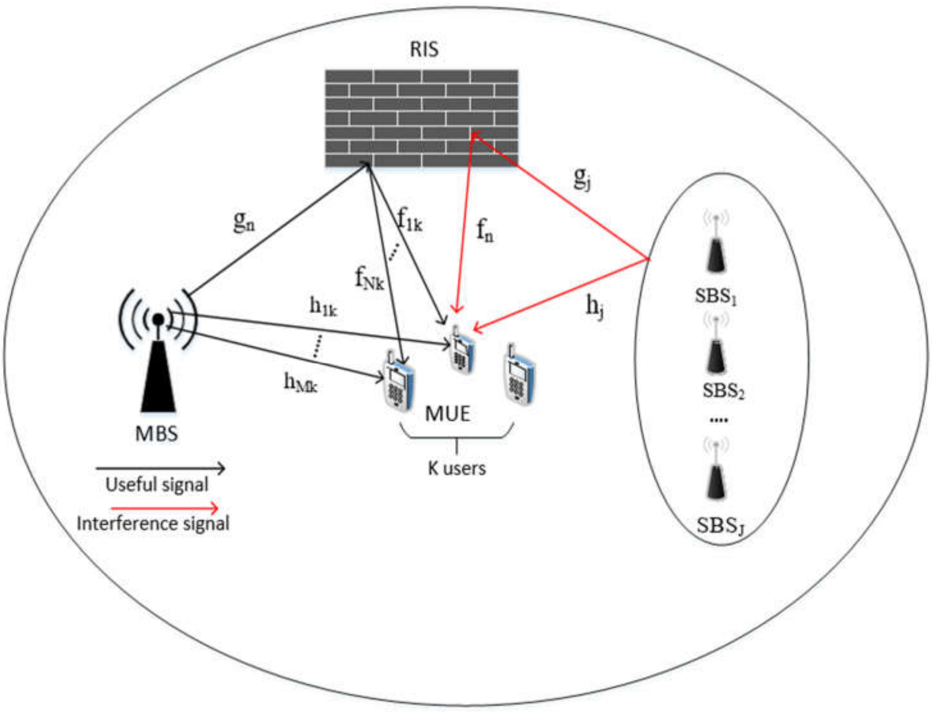

Figure 1. RIS-assisted HetNet system.

Preprints (www.preprints.org) | NOT PEER-REVIEWED | Posted: 10 May 2023 doi:10.20944/preprints202305.0689.v1

The SBSs installed within the MBS network causes MBS users to experience cross-tier interference. RIS is deployed in the network to enable interference mitigation. Let the channel coefficient vector between the MBS and the k-th macrocell user (MUE) is defined as $h_k = [h_{1k}, \dots, h_{Mk}]^T \in \mathbb{C}^{1\times M}$, where the direct channel coefficient matrix from the M MBS antennas to the K MBS users is $H = [h_1| \dots .|h_K] \in \mathbb{C}^{M\times K}$ for $m = 1, \dots M$, and $k = 1, \dots K$. The channel coefficient vector between the MBS and a RIS, as well as between RIS and the k-th macrocell user is represented as $g_n = [g_{1n}, \dots, g_{Mn}]^T \in \mathbb{C}^{M\times 1}$, where $G = [g_1| \dots |g_N] \in \mathbb{C}^{M\times N}$ is the channel coefficient matrix from the M MBS antennas to the RIS, and $f_k = [f_{1k}, \dots, f_{Nk}]^T \in \mathbb{C}^{1\times N}$, respectively, where $F = [f_1| \dots |f_K] \in \mathbb{C}^{N\times K}$ is the channel coefficient matrix between the RIS and all of the macrocell users, for $n = 1, \dots, N$. The channel coefficient vector from the SBSs to the k-th MUE is denoted as $h_j = [h_{1k}, \dots, h_{Jk}]^T \in \mathbb{C}^{1\times J}$, where the matrix of the direct channel between the SBSs and MUE is $H^S = [h_1| \dots |h_J] \in \mathbb{C}^{J\times K}$ for $j = 1, \dots J$, and the reflected channel coefficient vector from the SBSs to the RIS is denoted as $g_j = [g_{1n}, \dots, g_{Jn}] \in \mathbb{C}^{J\times 1}$, where $G_S = [g_1| \dots |g_J] \in \mathbb{C}^{J\times N}$ is the channel coefficient matrix between the SBSs and the RIS. The reflected interference channel vector from the SBSs-RIS link to the MUE is denoted as $f_n = [f_{1k}, \dots, f_{Nk}]^T \in \mathbb{C}^{1\times N}$. The signal of the MBS is $x_m = \sqrt{P_m}x_k$, and the signal of the SBS is $x_s = \sum_{j=1}^{J}\sqrt{P_j}x_j$. Let's define the phase shift matrix as a diagonal matrix as well $\Theta = \mathrm{diag}(\theta_1, \theta_2, \dots, \theta_N)$, where $\theta_n \in [0, 2\pi]$ is the phase shift at the nth element, where $\theta_N = \beta_n e^{j\theta_n}$ comprises an amplitude coefficient $\beta_n \in [0,1]$. Since we aim to obtain the maximum designed signal, we set the amplitude coefficient as $\beta_n = 1$. Hence, the received signal at the k-MUE can be written as

$$y_k = (h_k{}^T + f_k^T \Theta g_n)\sqrt{P_m}x_k + (h_j{}^T + f_n^T \Theta g_j)\sum_{j=1}^{J}\sqrt{P_J}x_j + \varepsilon \quad (1)$$

Where x_k and x_j are the MBS and SBS transmitted signals, respectively, and ε is the noise which follows $\mathcal{CN}(0, \sigma^2)$. The transmission signals of the MBS and SBS satisfy $E[|x_k|^2] = 1$ and $E\left[|x_j|^2\right] = 1$. Using (1), the signal noise ratio at the k-th MUE is expressed as

$$SNR_k = \frac{P_m|h_k{}^T + f_k^T \Theta g_n|^2}{\sum_{j=1\ j\neq n\ j\neq k}^{J} P_j|h_j{}^T + f_n^T \Theta g_j|^2 + \sigma^2} \quad (2)$$

Where P_m and P_j are the MBS and SBS transmitted power, respectively. Based on (2) the achievable rate of the k-th MUE, which is formulated as

$$R_k = \log_2(1 + SNR_k) \quad (3)$$

4. Problem Formulation

Our objective is to maximize the sum rate of the network by jointly optimizing the transmit beamforming w and the phase shift matrix Θ, which can be represented as

$$\text{(P1):}\ \max_{W,\Theta} \sum_{k=1}^{K} R_k \quad \text{(4a)}$$

$$\text{Subject to} \quad \sum_{k=1}^{K} \|w_k\| \leq P, \quad \text{(4b)}$$

$$0 \leq \theta_n \leq 2\pi \ , \ n = 1, \dots . N \qquad \text{(4c)}$$

The optimization problem in (4) is non convex because of the optimization variables and the non-convex constrains in (4c). We adapt Zero-Forcing-based transmit beamforming $W = \frac{(H^T + F^T \Theta G)^T}{(H^T + F^T \Theta G)(H^T + F^T \Theta G)^T}$, to the MBS to simplify the problem (4). In addition, the obtained transmit beamforming vector must be normalized by a factor of $\frac{\sqrt{P_m}(H^T + F^T \Theta G)^T}{\|H^T + F^T \Theta G\|}$ to fulfill the power constraint in (4b). Accordingly, due to the non-concave objective function in (4), we propose to

Preprints (www.preprints.org) | NOT PEER-REVIEWED | Posted: 10 May 2023 doi:10.20944/preprints202305.0689.v1

maximize the sum of the combined desired channel gain (CDC) of the MUE and the problem in (4) can be represented solely in terms of Θ , which is formulated as

$$\max_{\Theta} \sum_{k=1}^{K} \left| h_k{}^T + f_k^T \Theta g_n \right|^2 \quad (5a)$$

$$\text{Subject to } \; 0 \leq \theta_n \leq 2\pi \,, \forall_n \quad (5b)$$

4.1. RIS reflecting coefficient-based Optimization (RCO)

Now, we perform the optimization over the reflecting coefficient Θ, and with the fixed W, problem (4a) is reduced into (5a). To facilitate design, let's adopt a relaxation method to solve the problem (5a) efficiently.

Defining $A = diag(f_k^T) \times g_n$, $\phi = [\phi_1, \quad \phi_2, \dots, \quad \phi_n]^T$, where $\phi_n = e^{j\theta_n}$, (5b) becomes $|\phi_n| = 1, \forall_n$ (6)

Problem (5) becomes

$$\max_{\phi} \sum_{k=1}^{K} \phi^T A A^T \phi + \phi^T A h_k + h_k^T A^T \phi + \|h_k^T\|^2 \quad (7a)$$

$$\text{Subject to } \; |\phi_n|^2 = 1, \forall_n \quad (7b)$$

Problem (7) is a non convex quadratically constrained programme (QCQP) problem [27], it can be changed by adding an auxiliary variable t to become a homogenous QCQP problem.

$$\max_{\bar{\phi}} \sum_{k=1}^{K} \bar{\phi}^T B \bar{\phi} + \|h_k^T\|^2 \quad (8a)$$

$$\text{Subject to } \; |\overline{\phi_n}| = 1, \; \forall_n \quad (8b)$$

Where $B = \begin{bmatrix} AA^T & Ah_k \\ h_k^T A^T & 0 \end{bmatrix}$, and $\bar{\phi} = \binom{\phi}{t}$ (9)

But problem (8) is still non-convex, define $V = \bar{\phi}\bar{\phi}^T$, which must satisfy $rank(V) = 1$, note that $\bar{\phi}^T B \bar{\phi} = trace\,(BV)$. Thus, problem (8) becomes

$$\max_{V} \sum_{k=1}^{K} trace\,(BV) + \|h_k^T\|^2$$

$$\text{Subject to } \; V_{n,n} = 1, \forall_n \quad (10)$$

As problem (10) is a convex SDP problem, it can be solved by using the convex optimization tool such as CVX [27].

5. Simulation Results

5.1. Simulation Setup

The MBS is deployed at the origin point (0,0), the RIS is located at the coordinates (50,0), and the location of the K-MUE is determined randomly based on the uniform distribution in a (100,100) rectangular space as illustrated in Fig. 2. We assume the direct propagation path between an MBS and a MUE is dominated by non-line-of-site (NLOS) components and, as a result, follows Rayleigh fading. But because we assume that the RIS is positioned so that it is free of any obstructions and has LOS coverage with both MBS, and MUE, RIS-related channels adhere to Rician fading [5]. The simulation setup is shown in the Fig.2.

Preprints (www.preprints.org) | NOT PEER-REVIEWED | Posted: 10 May 2023 doi:10.20944/preprints202305.0689.v1

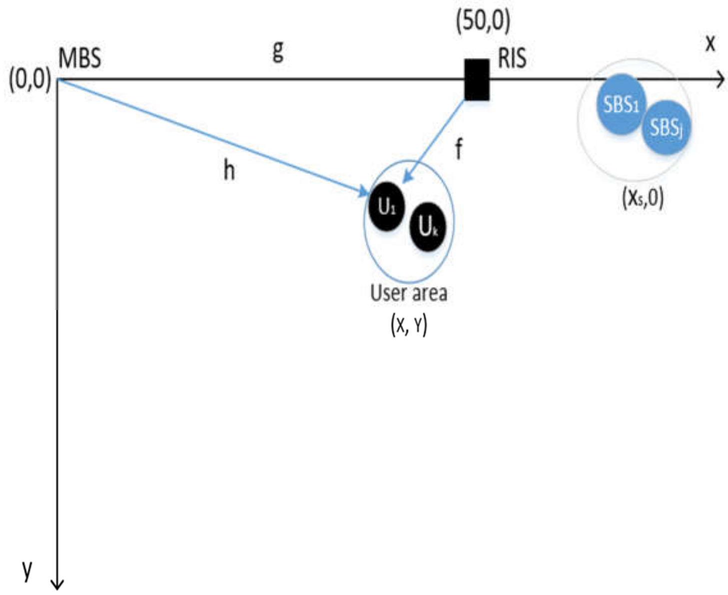

Figure 2. Simulation setup.

The coverage radius of the macrocell and small cell are 500m and 20m [21], respectively. The distance-dependent path loss factor is given by [5]

$$L(d) = C_0 \left(\frac{d}{D_0}\right)^{-\alpha} \quad (11)$$

C_0 represents the pathloss at the reference distance, $D_0 = 1m$, d is the distance between the MBS and MUE, and α is the pathloss exponent. Specifically, the small-scale channel from the MBS to the RIS can be expressed as [10]

$$G_m = \sqrt{\frac{\Omega}{\Omega+1}}\overline{H_m} + \sqrt{\frac{1}{\Omega+1}}\widehat{H_m} \qquad (12)$$

Where Ω is the Rician factor, and $\overline{H_m}$ and $\widehat{H_m}$ are the LOS and NLOS components, respectively. The channel between the RIS and the k-th MUE f_m is also subject to the same channel model, and it is modelled as [10]

$$f_m = \sqrt{\frac{\Omega}{\Omega+1}}\overline{f_m} + \sqrt{\frac{1}{\Omega+1}}\widehat{f_m} \qquad (13)$$

The distance between the MBS and RIS is 50m. The distance between RIS and MUE is 5m [21]. The detailed parameter setting is shown in Table 1.

Table 1: System parameters

Parameters	Values
S	4
K	2
J	4
Center frequency	5GHz[5]
σ^2	-60dBm[7]
α	3[21]
Ω	10[7]
P_j	26 dBm [1]
P_m	40 dBm[1]
M	4
C_0	-30dBm [5]

Preprints (www.preprints.org) | NOT PEER-REVIEWED | Posted: 10 May 2023 doi:10.20944/preprints202305.0689.v1

Now, in order to assess the effectiveness of the proposed HetNet networks scheme, we compare its SE performance to two reference scenarios:

- **Random phase shift**: In this example, we choose the phase shift at random in the range $[0, 2\pi]$, and then we execute zero-forcing (ZF) at the MBS using the combined channel [5], [7].
- **Absent RIS (without RIS)**: In this plan, we mimic the network without RIS deployment. As a result, only the direct propagation path is included in the signal that the MUE has received.

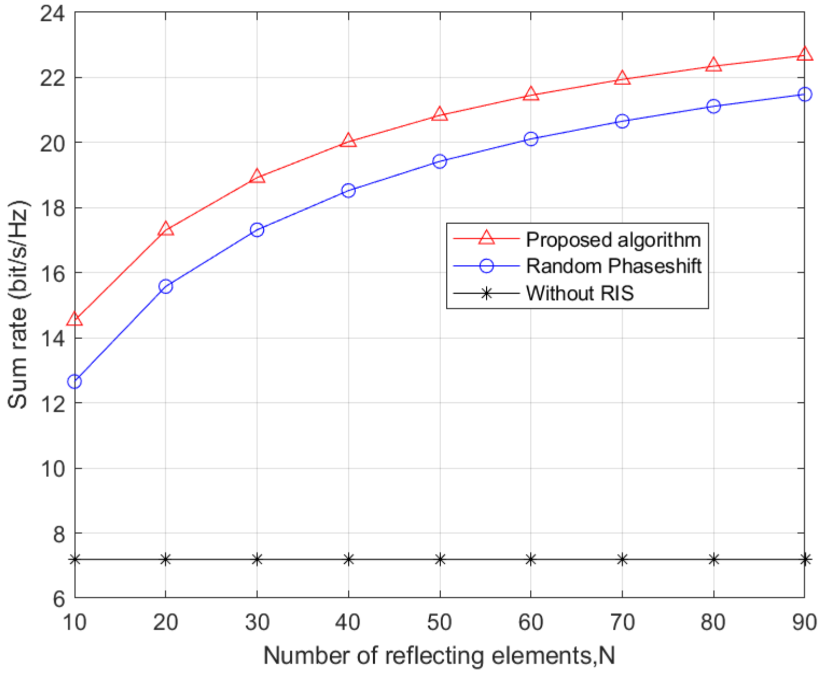

Figure 1. Sum rate vs number of element for d= 50 m

In Fig. 3, we evaluate the sum rate versus the number of elements of the RIS. It can be seen that the proposed scheme can achieve a higher performance gain compared to the other benchmarks. With an increasing number of RIS elements, the sum rate increases. This is not the case for the method without RIS, which is not impacted by the number of RIS elements. There is only a slight gain when compared to the random phase shift approach. This shows that using passive beamforming via RCO in a RIS-assisted HetNet network can mitigate cross-tier interference and increase the system sum rate.

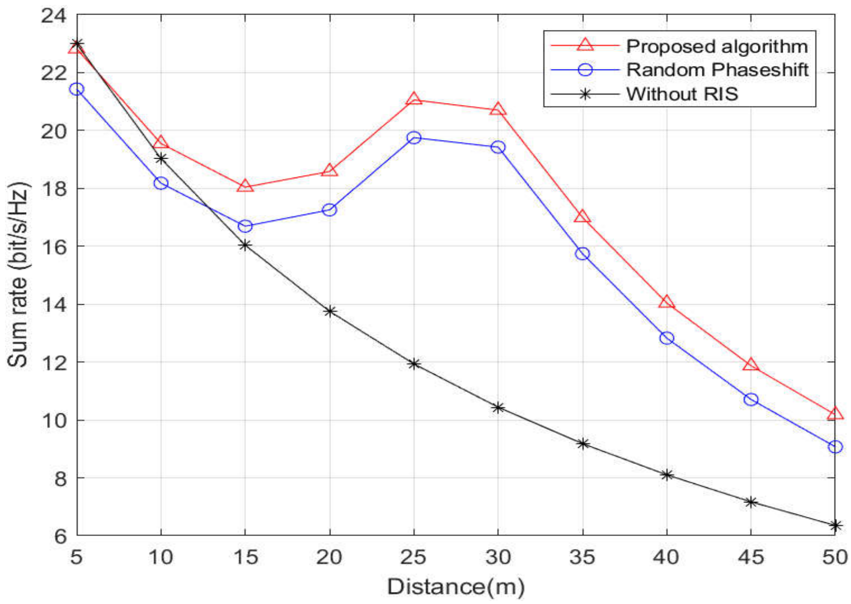

Figure 2. Distance vs the sum rate N = 50

Preprints (www.preprints.org) | NOT PEER-REVIEWED | Posted: 10 May 2023 doi:10.20944/preprints202305.0689.v1

Next, in Fig. 4, we compare the sum rate required by all schemes versus the distance between the MBS and the MUE. Specifically, we alter the distance between MBS and MUE while keeping the placement of RIS constant.

In the scenarios without RIS, it is first noted that the total rate drops as the distance increases. This is due to the pathloss that depends on distance. Second, we observed how the network performs with RIS support. As the distance grows, it is shown that the total rate first declines, then increases to achieve an ideal value before decreasing once more. Following is an explanation for this. When the MUE and MBS are close, the MBS's direct path takes precedence over the reflected path. However, when the distance grows, the reflected path begins to trump the direct path. At this stage, we can see that the proposed technique outperforms the random situation. The RCO, in particular, gives a superior solution for the phase shift at a distance of 25m.

It is possible to deduce that deploying RIS can enhance the total rate of the RIS-assisted HetNet if the distance between RIS and MUE is between 24-34m.

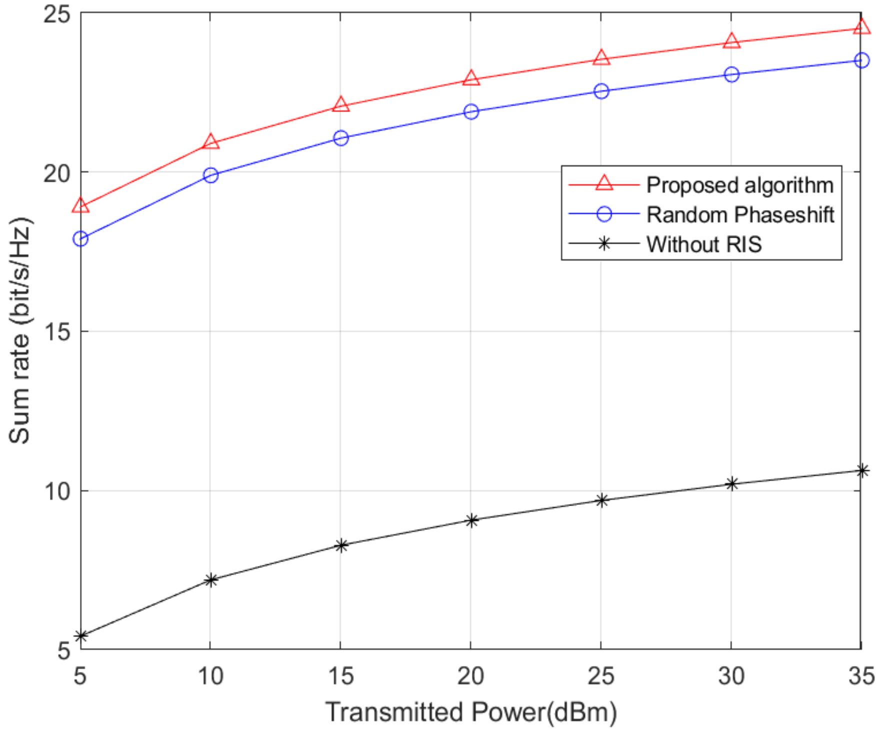

Figure 3. Transmit power versus sum rate N = 50, d =50m

Figure 5 depicts the total rate performance in relation to the MBS transmitted power. The chart shows that, for any given transmit power, the proposed scheme produces a substantially greater total rate than the other two schemes. This indicates the efficiency of implementing RIS in a heterogeneous network (HetNet).

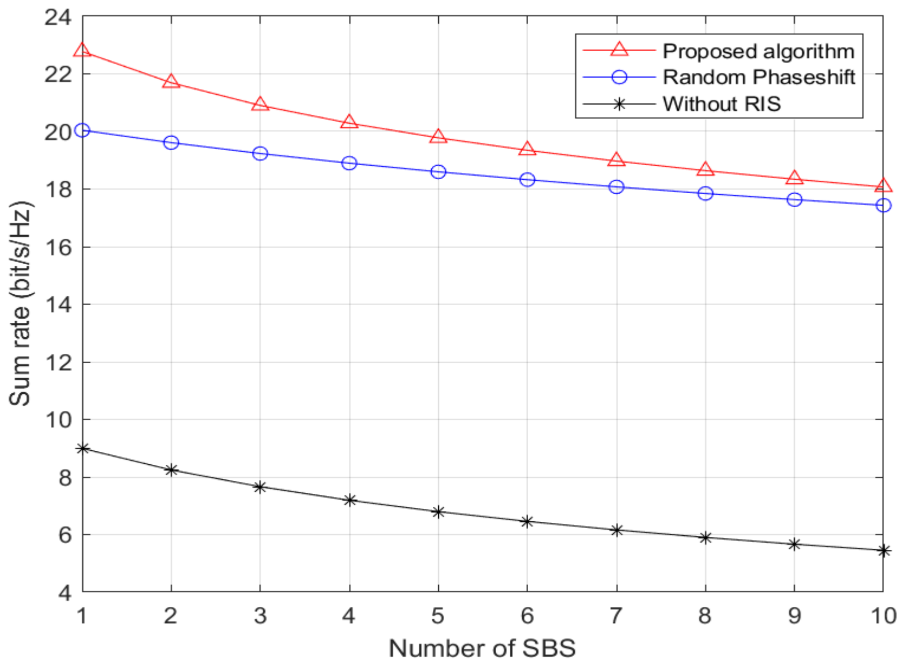

Figure 4. Number of SBS vs sum rate N= 50 and d =50m

Finally, in Fig. 6, we show the total rate for an increasing number of small base stations (SBS). The chart shows that the suggested scheme outperforms the baseline scheme in terms of sum rate. Furthermore, as the number of SBS increases, the network's performance drops. This is due to an increase in the number of SBS transmitters. The decrease also reflects that passive beamforming at the RIS via proper phase shift design can alleviate the interference caused by the increased number of small base stations (SBS).

6. Conclusions

There has been surprisingly rising research and development activity on the reconfigurable intelligent surfaces (RIS) topic from both academia and industry working in antenna design, metamaterials, electromagnetics, signal processing, and wireless communications as a result of the increased potential of reconfigurable intelligent surfaces for wireless communications, as witnessed by the various recent proofs of concepts ranging from reflect arrays to intelligent antennas. Recently, the use of RIS in wireless communications networks has been promoted as a revolutionary method for transforming any wireless signal propagation environment into one that can be dynamically programmed for a variety of networking goals, such as coverage extension, environmental perception, sensing, spatiotemporal focusing, and interference mitigation. In this paper, we have discussed an RIS-assisted HetNet to maximize the sum rate for macrocell users (MUE). With respect to the total transmit beamforming constraint and realistic phase shift concerns, the MBS's transmit beamforming and the RIS's phase shifts were simultaneously optimised. To address the unconvex problem, we first adapted zero-forcing-based transmit beamforming to simplify the problem, and then we proposed to maximize the sum rate of the combined desired channel gain by efficiently applying reflection coefficient-based optimization (RCO). The effectiveness of the suggested system was demonstrated by the simulation results, which also offered some useful insights into how to deploy RIS to obtain the ideal sum rate values in HetNet. Finally, we have substantiated from the simulation results that an RIS can enhance the performance and reliability of HetNet systems.

Data Availability: The data used to support the findings of this study are available from the corresponding author upon request.

Conflicts of Interest: The authors declare no conflict of interest.

Acknowledgments: This work is supported by the African Union (AU).

References

1. A. Nasser, O. Muta, M. Elsabrouty, and H. Gacanin, "Interference Mitigation and Power Allocation Scheme for Downlink MIMO-NOMA HetNet," *IEEE Trans Veh Technol*, vol. 68, no. 7, pp. 6805–6816, Jul. 2019, doi: 10.1109/TVT.2019.2918336.
2. A. Nasser, O. Muta, H. Gacanin, and M. Elsabrouty, "Non-Cooperative Game Based Power Allocation for Energy and Spectrum Efficient Downlink NOMA HetNets," *IEEE Access*, vol. 9, pp. 136334–136345, 2021, doi: 10.1109/ACCESS.2021.3116706.
3. M. U. Iqbal, E. A. Ansari, and S. Akhtar, "Interference mitigation in hetnets to improve the QoS using q-learning," *IEEE Access*, vol. 9, pp. 32405–32424, 2021, doi: 10.1109/ACCESS.2021.3060480.
4. A. Y. Kassim, A. M. S Tekanyi, H. A. Abdulkareem, Z. Z. Muhammad, M. D. Almustapha, and U. F. Abdu-Aguye, "AN IMPROVED CROSS-TIER INTERFERENCE MITIGATION SCHEME IN A FEMTO-MACRO HETEROGENEOUS NETWORK," 2020.
5. A. Mondal, A. M. H. Al Junaedi, K. Singh, and S. Biswas, "Spectrum and Energy-Efficiency Maximization in RIS-Aided IoT Networks," *IEEE Access*, vol. 10, pp. 103538–103551, 2022, doi: 10.1109/ACCESS.2022.3209823.
6. K. V. Mishra, A. Chattopadhyay, S. S. Acharjee, and A. P. Petropulu, "OptM3Sec: Optimizing Multicast IRS-Aided Multiantenna DFRC Secrecy Channel with Multiple Eavesdroppers," Jan. 2022, [Online]. Available: http://arxiv.org/abs/2201.09436
7. S. Jiao, X. Xie, and Z. Ding, "Deep Reinforcement Learning-Based Optimization for RIS-Based UAV-NOMA Downlink Networks (Invited Paper)," *Frontiers in Signal Processing*, vol. 2, Jul. 2022, doi: 10.3389/frsip.2022.915567.
8. M. Jian *et al.*, "Reconfigurable intelligent surfaces for wireless communications: Overview of hardware designs, channel models, and estimation techniques," *Intelligent and Converged Networks*, vol. 3, no. 1, pp. 1–32, Apr. 2022, doi: 10.23919/icn.2022.0005.
9. W. Mei, B. Zheng, C. You, and R. Zhang, "Intelligent Reflecting Surface Aided Wireless Networks: From Single-Reflection to Multi-Reflection Design and Optimization," Sep. 2021, [Online]. Available: http://arxiv.org/abs/2109.13641
10. Q. Wu and R. Zhang, "Intelligent Reflecting Surface Enhanced Wireless Network via Joint Active and Passive Beamforming," in *IEEE Transactions on Wireless Communications*, Institute of Electrical and Electronics Engineers Inc., Nov. 2019, pp. 5394–5409. doi: 10.1109/TWC.2019.2936025.
11. M. Di Renzo *et al.*, "Smart Radio Environments Empowered by Reconfigurable Intelligent Surfaces: How It Works, State of Research, and the Road Ahead," *IEEE Journal on Selected Areas in Communications*, vol. 38, no. 11, pp. 2450–2525, Nov. 2020, doi: 10.1109/JSAC.2020.3007211.
12. R. Fara, P. Ratajczak, D.-T. Phan-Huy, A. Ourir, M. Di Renzo, and J. De Rosny, "A Prototype of Reconfigurable Intelligent Surface with Continuous Control of the Reflection Phase Modeling, Full-Wave Electromagnetic Characterization, Experimental Validation, and Application to Ambient Backscatter Communications."
13. D. Pérez-Adán, Ó. Fresnedo, J. P. Gonzalez-Coma, and L. Castedo, "Intelligent reflective surfaces for wireless networks: An overview of applications, approached issues, and open problems," *Electronics (Switzerland)*, vol. 10, no. 19, Oct. 2021, doi: 10.3390/electronics10192345.
14. X. Pei *et al.*, "RIS-Aided Wireless Communications: Prototyping, Adaptive Beamforming, and Indoor/Outdoor Field Trials," Feb. 2021, [Online]. Available: http://arxiv.org/abs/2103.00534
15. M. Di Renzo *et al.*, "Reconfigurable intelligent surfaces vs. relaying: Differences, similarities, and performance comparison," *IEEE Open Journal of the Communications Society*, vol. 1, pp. 798–807, 2020, doi: 10.1109/OJCOMS.2020.3002955.
16. N. A. Kamaruddin, A. Mahmud, M. Y. Bin Alias, A. Abd Aziz, and S. Yaakob, "Performance Evaluation of Reconfigurable Intelligent Surface against Distributed Antenna System at the Cell Edge," *Electronics (Basel)*, vol. 11, no. 15, p. 2376, Jul. 2022, doi: 10.3390/electronics11152376.
17. E. Björnson, Ö. Özdogan, and E. G. Larsson, "Intelligent Reflecting Surface vs. Decode-and-Forward: How Large Surfaces Are Needed to Beat Relaying?," Jun. 2019, doi: 10.1109/LWC.2019.2950624.

 doi:10.20944/preprints202305.0689.v1

18. X. Guan, Q. Wu, and R. Zhang, "Joint Power Control and Passive Beamforming in IRS-Assisted Spectrum Sharing," *IEEE Communications Letters*, vol. 24, no. 7, pp. 1553–1557, Jul. 2020, doi: 10.1109/LCOMM.2020.2979709.
19. B. Agarwal, M. A. Togou, M. Ruffini, and G. M. Muntean, "Mitigating the Impact of Cross-Tier Interference on Quality in Heterogeneous Cellular Networks," in *Proceedings - Conference on Local Computer Networks, LCN*, IEEE Computer Society, Nov. 2020, pp. 497–502. doi: 10.1109/LCN48667.2020.9314834.
20. K. Sundaresan and S. Rangarajan, "Cross-tier interference mitigation considering pilot overhead for TDD MIMO heterogeneous networks," *Proc. ACM Intl. Symp. Mobile Ad Hoc Netw. Comput*, vol. 19, no. 2, pp. 3590–3600, 2015, doi: 10.1109/GLOCOM.2015.
21. X. Yongjun *et al.*, "Resource Allocation for Two-Tier RIS-Assisted Heterogeneous NOMA Networks," *ZTE Communications*, vol. 20, no. 1, pp. 36–47, 2022, doi: 10.12142/ZTECOM.202201006.
22. Y. Bian, D. Dong, J. Jiang, and K. SONG, "Performance Analysis of Reconfigurable Intelligent Surface-Assisted Wireless Communication Systems under Co-Channel Interference," *IEEE Open Journal of the Communications Society*, 2023, doi: 10.1109/OJCOMS.2023.3244648.
23. W. Jiang and H. Schotten, "Orthogonal and Non-Orthogonal Multiple Access for Intelligent Reflection Surface in 6G Systems," Mar. 2023, [Online]. Available: http://arxiv.org/abs/2303.08825
24. F. C. Okogbaa *et al.*, "Design and Application of Intelligent Reflecting Surface (IRS) for Beyond 5G Wireless Networks: A Review," *Sensors*, vol. 22, no. 7, p. 2436, Mar. 2022, doi: 10.3390/s22072436.
25. A. Danish and N. Farhan, "Impact of Amplitude Response on the Capacity of an Intelligent-Reflecting-Surface-Enabled Narrowband SISO System," in *INTERACT 2023*, Basel Switzerland: MDPI, Apr. 2023, p. 2. doi: 10.3390/engproc2023032002.
26. I. Hameed, M. R. Camana, P. V. Tuan, and I. Koo, "Intelligent Reflecting Surfaces for Sum-Rate Maximization in Cognitive Radio Enabled Wireless Powered Communication Network," *IEEE Access*, vol. 11, pp. 16021–16031, 2023, doi: 10.1109/ACCESS.2023.3243848.
27. A. M. C. So, J. Zhang, and Y. Ye, "On approximating complex quadratic optimization problems via semidefinite programming relaxations," *Math Program*, vol. 110, no. 1, pp. 93–110, Jun. 2007, doi: 10.1007/s10107-006-0064-6.